

Original Article  
Oncology



# 3D-culture models as drug-testing platforms in canine lymphoma and their cross talk with lymph node-derived stromal cells

Ju-Hyun An <sup>1</sup>, Woo-Jin Song <sup>2</sup>, Qiang Li <sup>3</sup>, Dong-Ha Bhang <sup>4,\*</sup>,  
Hwa-Young Youn <sup>1,\*</sup>

<sup>1</sup>Laboratory of Veterinary Internal Medicine, College of Veterinary Medicine, Seoul National University, Seoul 08826, Korea

<sup>2</sup>Laboratory of Veterinary Internal Medicine, College of Veterinary Medicine, Jeju National University, Jeju 63243, Korea

<sup>3</sup>Department of Veterinary Medicine, College of Agriculture, Yanbian University, Yanji 133000, China

<sup>4</sup>Department of Molecular Cell Biology, Samsung Biomedical Research Institute, Sungkyunkwan University School of Medicine, Suwon 16419, Korea

 OPEN ACCESS

Received: Oct 14, 2020

Revised: Jan 4, 2021

Accepted: Feb 1, 2021

\*Corresponding authors:

Hwa-Young Youn

Laboratory of Veterinary Internal Medicine,  
College of Veterinary Medicine, Seoul National  
University, 1 Gwanak-ro, Gwanak-gu, Seoul  
08826, Korea.

E-mail: hyyoun@snu.ac.kr

Dong-Ha Bhang

Department of Molecular Cell Biology,  
Samsung Biomedical Research Institute,  
Sungkyunkwan University School of Medicine,  
2066 Seobu-ro, Jangan-gu, Suwon 16419,  
Korea.

E-mail: angd77@gmail.com


© 2021 The Korean Society of Veterinary  
Science

This is an Open Access article distributed  
under the terms of the Creative Commons  
Attribution Non-Commercial License ([https://  
creativecommons.org/licenses/by-nc/4.0](https://creativecommons.org/licenses/by-nc/4.0))  
which permits unrestricted non-commercial  
use, distribution, and reproduction in any  
medium, provided the original work is properly  
cited.

ORCID iDs

Ju-Hyun An 

<https://orcid.org/0000-0002-3756-9482>

Woo-Jin Song 

<https://orcid.org/0000-0001-9563-6615>

## ABSTRACT

**Background:** Malignant lymphoma is the most common hematopoietic malignancy in dogs, and relapse is frequently seen despite aggressive initial treatment. In order for the treatment of these recurrent lymphomas in dogs to be effective, it is important to choose a personalized and sensitive anticancer agent. To provide a reliable tool for drug development and for personalized cancer therapy, it is critical to maintain key characteristics of the original tumor.

**Objectives:** In this study, we established a model of hybrid tumor/stromal spheroids and investigated the association between canine lymphoma cell line (GL-1) and canine lymph node (LN)-derived stromal cells (SCs).

**Methods:** A hybrid spheroid model consisting of GL-1 cells and LN-derived SC was created using ultra low attachment plate. The relationship between SCs and tumor cells (TCs) was investigated using a coculture system.



**Results:** TCs cocultured with SCs were found to have significantly upregulated multidrug resistance genes, such as *P-gp*, *MRPI*, and *BCRP*, compared with TC monocultures. Additionally, it was revealed that coculture with SCs reduced doxorubicin-induced apoptosis and G2/M cell cycle arrest of GL-1 cells.

**Conclusions:** SCs upregulated multidrug resistance genes in TCs and influenced apoptosis and the cell cycle of TCs in the presence of anticancer drugs. This study revealed that understanding the interaction between the tumor microenvironment and TCs is essential in designing experimental approaches to personalized medicine and to predict the effect of drugs.

**Keywords:** Canine lymphoma; lymph node-derived stromal cell; drug resistance; personalized cancer therapy; tumor microenvironment

## INTRODUCTION

Malignant lymphoma is the most common hematopoietic malignancy in dogs, and this neoplastic disease is controllable by aggressive chemotherapy with a doxorubicin (DOX)-

Qiang Li <https://orcid.org/0000-0002-6876-9460>Dong-Ha Bhang <https://orcid.org/0000-0002-6727-4036>Hwa-Young Youn <https://orcid.org/0000-0002-0283-1348>

#### Funding

This study was supported by the Research Institute for Veterinary Science, Seoul National University. In addition, this research was supported by Basic Science Research Program through the National Research Foundation of Korea (NRF) funded by the Ministry of Education (550-20190038). These funds contributed to the collection, analysis, and interpretation of data in this study.

#### Conflict of Interest

The authors declare no conflicts of interest.

#### Author Contributions

Conceptualization: An JH, Song WJ, Li Q, Bhang DH, Youn HY; Data curation: An JH, Song WJ, Li Q, Bhang DH, Youn HY; Formal analysis: An JH, Bhang DH, Youn HY; Funding acquisition: Bhang DH, Youn HY; Investigation: An JH, Bhang DH, Youn HY; Methodology: An JH; Project administration: Bhang DH, Youn HY; Resources: An JH, Bhang DH, Youn HY; Software: Bhang DH, Youn HY; Supervision: Bhang DH, Youn HY; Validation: Bhang DH, Youn HY; Visualization: Bhang DH, Youn HY; Writing - original draft: An JH; Writing - review & editing: An JH, Bhang DH, Youn HY.

based multidrug chemotherapy protocol, which results in a high rate of remission [1]. However, relapse is frequently seen despite the aggressive initial treatment [2], leading to treatment failure and ultimately the dog's death [3]. Treatment failure can be attributed to tumor drug resistance (DR), which can occur during the onset of chemotherapy (intrinsic DR) or during chemotherapy (or acquired DR) [4]. When such resistance develops, even patients with the same type of disease can have very different tumor phenotypes and sensitivity to anticancer drugs [5]. Therefore, in order to choose an effective treatment for dogs with recurrent lymphoma, it is important to choose a personalized and sensitive anticancer agent [6]. Traditionally, cells grown in monolayers have been used as disease models for cell biology research and drug screening, and these 2-dimensional (2D) models are assumed to reflect actual tissue physiology [7]. However, 2D cell culture lacks important functions to revive physiological systems such as spatial cell-cell interactions, the presence of extracellular matrix (ECM), dynamic metabolic demands, and increased hypoxia due to mass growth [8]. For this reason, it is now recognized that 2D-cultured cells cannot simulate the microenvironment of the original tumor. Many drugs that have proven clinically futile have been preclinically evaluated as “active” using a 2D-cultured cell line model [9]. In contrast, 3-dimensional (3D) cell culture spheroids are self-assembled cell aggregates that recapitulate many important characteristics of physiological spatial growth and cell-cell interaction [10]. In large spheroids, which can reach up to 500  $\mu\text{m}$  in diameter, cells in the outer layer continue to multiply, while hypoxia and malnutrition cause necrosis of the core [11]. These conditions are similar to hypoxic microtumors *in vivo*, which are known to negatively affect the tumor's sensitivity to anticancer drugs and contribute to acquired resistance [12]. As a result, 3D cell culture techniques more similar to the *in vivo* cell environment are now being pursued intensely, as it is expected to yield better precision in drug discovery [13].

DelNero et al. [14] identified similar changes, which they concluded were an effect of heterogeneous oxygen distribution during growth in the 3D culture system. Thus, it is important to investigate hypoxia and tissue level effects in 3D tumor models [14]. Hypoxia activates a response program that is largely controlled by the transcription factor hypoxia inducible factor 1 (HIF-1) [14]. Other studies have shown that HIF-induced upregulation of angiogenic morphogens, including vascular endothelial growth factor (*VEGF*) and basic fibroblast growth factor (*bFGF*), promotes angiogenesis. Additionally, these factors have been shown to act not only as promoters of proliferation and inhibitors of apoptosis in cancer cells but also as enhancers of drug resistance [15].

Hypoxia has been considered as a major feature of the tumor microenvironment and as a potential contributor to drug resistance and is recapitulated in 3D cell culture models [16]. Drug resistance is one of the major reasons for poor outcomes of high-risk therapies and recurrent lymphoma. The ABC proteins such as P-glycoprotein (*P-gp*), breast cancer resistance protein (*BCRP*), and multi-drug resistance (MDR)-related protein (*MRP1*) bind ATP and use the energy to drive the transport of various molecules across the plasma membrane. As they can eliminate anticancer drugs from cells, they contribute to drug resistance [17]. However, as the microenvironment around tumors interacts with the tumor cells (TCs) and various stromal cells (SCs), 3D spheroids composed of single TCs have limitations in representing the tumor microenvironment [18].

Growth of TCs in the presence of SCs is thought to better mimic the microenvironment of the tumor *in vivo* [19]. Previous studies have shown that the complex interconnection between TCs and SCs changes the gene expression profile of SCs as well as their activation status,

which initiates angiogenesis and contributes to drug resistance in TCs [12]. However, studies on the relationship between lymphoid-derived TCs and SCs in veterinary medicine are still insufficient. Furthermore, as lymphocytes are generally mobile, it is assumed that stromal populations firmly support the distribution and movement of lymphocytes within structural skeletons of the lymph node (LN) [20].

The first goal of the current study was to evaluate the differences between 2D and 3D cell cultures of TCs (lymphoma cell line) when treated with chemotherapeutic drugs. DOX was selected based on previous studies of resistance in human TCs and its effectiveness in treating dog lymphoma. Furthermore, due to the importance of the microenvironment produced by SCs in anticancer sensitivity and anticancer drug resistance of TCs, we established a hybrid tumor/stroma spheroid 3D model. The final goal of this study was to clarify the role of canine LN-derived SCs in lymphoma GL-1 cell line survival and proliferation during anticancer drug treatment and to assess the expression of the ABC-transporter *P-gp*, *MRPI*, and *BCRP* in GL-1 cell lines cocultured with SCs.

## MATERIALS AND METHODS

### LN-derived SC isolation

SCs were isolated from submandibular LN obtained from three healthy beagle dogs. All animal experiments in this study were approved by the institutional animal care and use committee of Seoul National University (SNU), Republic of Korea, and all protocols were in accordance with the approved guidelines (SNU, protocol No. SNU-1881112-2). Tissue was obtained from LNs via needle biopsy. Tissues were washed three times with Dulbecco's phosphate-buffered saline (DPBS; PAN-Biotech, Germany) containing 1% penicillin-streptomycin (PS; PAN-Biotech), plated on a Petri dish, digested with 0.1% Collagenase type 1A (Gibco/Life Technologies, USA) solution, and incubated for 50 min at 37°C in a humidified atmosphere of filtered 5% CO<sub>2</sub>. After digestion, Roswell Park Memorial Institute-1640 (RPMI-1640; Pan-Biotech) with 10% fetal bovine serum (FBS; Sigma-Aldrich, USA) and 1% PS was added to neutralize the sample. The sample was centrifuged at 1,200 × g for 5 min. The supernatant was discarded, the cell pellet was suspended in high-glucose Dulbecco's modified Eagle's Medium, and the suspension was passed through a 70 μm Falcon cell strainer (Thermo Fisher Scientific, USA) to remove debris. The suspension was centrifuged again at 1,200 × g for 5 min. Red blood cell lysis buffer (Sigma-Aldrich) was added, and the cell solution was incubated for 10 min at 25°C to remove erythrocytes. Cells were washed with five volumes of DPBS and centrifuged again. The supernatant was discarded, and then the cells were resuspended in RPMI-1640 and seeded (3,000/cm<sup>2</sup>) in cell culture dish. Unattached cells were removed the next day by washing with DPBS. Macrophages and DCs were eliminated from the culture, as they grew less or were harder to obtain by trypsinization and were therefore finally diluted out. In this experiment, 4–6 passages of SCs were used.

### Cell lines

GL-1 cell lines were received from Prof. Yuko Goto-Koshino (Tokyo University, Japan) and maintained in RPMI 1640 medium supplemented with 10% FBS in 5% CO<sub>2</sub> at 37°C. Its cytological and immunohistochemical properties are explained elsewhere [2,21].

### Flow cytometry

In this experiment, SCs between passage numbers 4 and 6 were used. SCs were harvested from culture dishes using trypsin. The cells were stained with antibodies by direct or indirect methods. The cells were analyzed using an FACSCalibur flow cytometer with CELLQuest software (Becton Dickinson, USA). Isolated SCs were evaluated by flow cytometry for the expression of SC markers such as CD90-PE (dilution, 1:200; Cat. No. 561970; BD Pharmingen, USA), CD73-PE (dilution, 1:200; Cat. No. 550741; BD Pharmingen), CD29 (dilution, 1:200; Cat. No. 555005; BD Pharmingen), CD34-PE (dilution, 1:200; Cat. No. 559369; BD Pharmingen), CD44 (dilution, 1:200, Cat. No. 11-5440-42; eBiosciences, USA), CD45 (dilution, 1:200; Cat. No. 11-5450-42; eBiosciences), CD31 (dilution, 1:200; Cat. No. PA5-16301; Invitrogen, USA), and Gp38 (dilution, 1:200; Cat. No. Orb76777; Biorbyt, UK). For CD31 and Gp38, indirect immunofluorescence was performed using mouse anti-rabbit IgG-PE (dilution, 1:200; Cat. No. sc-3753; Santa Cruz Biotechnology, USA) and goat anti-hamster IgG-FITC (dilution, 1:200; Cat. No. sc-2792; Santa Cruz Biotechnology), respectively. Unstained samples were used as the negative control. Characterization was conducted using FlowJo 7.6.5 software (TreeStar, Inc., USA).

### Spheroid formation using Petri dish well array

Stem FIT<sup>®</sup> 3D cell culture 25-well arrays (MICROFIT, Inc., Korea) were seeded with  $2.5 \times 10^5 - 2 \times 10^6$  cells per well of GL-1 cell lines. These cells were incubated in RPMI (PAN-Biotech) containing 20% FBS with 1% PS at 37°C for an additional 24 h to allow spheroid formation. For hybrid spheroid experiments, TCs were mixed in different ratios with LN SCs, consisting a total of  $2.5 \times 10^5$  cells per spheroid. TC:SC ratios used for this experiment were 1:0, 3:1, 1:1, 1:3 and 0:1. Spheroids were formed using the StemFIT<sup>®</sup> 3D cell culture dish templates as previously detailed. ImageJ (National Institutes of Health, USA, <http://imagej.nih.gov/ij/>) was used to calculate areas of the different spheroids as detailed in the spheroid image analysis section below.

### Histological analysis of spheroids

To visualize cell nuclei and cytoplasmic materials in spheroid samples (1:1 ratio of TC:SC), spheroids embedded in paraffin blocks were cut at a thickness of 3  $\mu$ m. The stain solutions were prepared according to manufacturer's specifications. The reagents used were as follows: Hematoxylin I (Thermo Fisher Scientific), Clarifier I (Thermo Fisher Scientific), Bluing Reagent (Thermo Fisher Scientific), and Eosin-Y (Thermo Fisher Scientific).

### Immunofluorescence analysis

To identify structures in SC hybrid spheroids, spheroids embedded in paraffin blocks (1:1 ratio of TC:SC) were cut at a thickness of 3  $\mu$ m. Sections were deparaffinized in xylene and rehydrated sequentially in 100%, 95%, and 80% ethanol solutions; antigen retrieval was carried out using 10 mM citrate buffer (Sigma-Aldrich). After washing, the sections were blocked with a blocking buffer containing 1% bovine serum albumin in PBST for 30 min. The sections were incubated overnight at 4°C with antibodies against CD79a (dilution, 1:50; Cat. No. MA5-13212; Invitrogen), CD31 (dilution, 1:50; Cat. No. PA5-16301; Invitrogen), or VE-cadherin (dilution, 1:50; Cat. No. SC-9989; Santa Cruz Biotechnology). After three washes, the slides were incubated with a secondary antibody. The sections, stained with an antibody against either CD79a, CD31 or VE-cadherin, were washed 3 times and incubated with mouse anti-rabbit IgG-PE (dilution, 1:200; Cat. No. sc-3753; Santa Cruz Biotechnology) and m-IgG $\kappa$  BP-CFL 488 (dilution, 1:200; Cat. No. sc-516176; Santa Cruz Biotechnology) for 1 h at room temperature in the dark. Then, sections were washed thrice and mounted in VECTASHIELD

mounting medium containing 4',6-diamidino-2-phenylindole (DAPI; Vector Laboratories, USA). The samples were visualized using EVOS FL microscope (Life Technologies, Germany), and the immunoreacted cells were counted in 20 random fields per group.

### Measurement of apoptosis

The percentage of apoptotic cells was determined by flow cytometry using the annexin V-FITC apoptotic detection kit (Cat. No. 556547; BD Pharmingen) following the manufacturer's protocol. Briefly, cells were washed twice with cold PBS and then resuspended in 1× binding buffer. Then, FITC-annexin V and PI (dilution, 1:20) were added to the cells and incubated for 15 min at 25°C in the dark. Subsequently, 400 µL 1× binding buffer was added to this sample. Flow cytometry was performed, and results were analyzed using FlowJo software.

### Anticancer drug treatment

Spheroids were grown in 96-well plates and treated with different concentrations of DOX (dose, 0, 0.05, and 0.5 µg/mL). Images of the spheroids were taken with a microscope on days 0, 1, 2, 3, 4, and 5. The images were analyzed using Image J.

### Quantitative reverse transcription polymerase chain reaction measurement

Total cellular RNA was extracted by Easy Blue total RNA extraction kit (iNtRON Biotechnology, Korea) according to the manufacturer's instruction. Then, cDNAs were synthesized from 1 µg of total RNA using the CellScript All-in-One 5× first strand cDNA synthesis Master Mix (CellSafe, Korea). Samples were evaluated in duplicate in 10 µL of AMPIGENE qPCR Green Mix Hi-ROX with SYBR Green dye (Enzo Life Sciences, USA) using 1 µL of cDNA and 400 nM each of forward and reverse primers (BIONICS, Korea). Expression was normalized to that of glyceraldehyde 3-phosphate dehydrogenase (*GAPDH*). The primer sequences are listed in **Table 1**.

### Trans well coculture system

TCs were plated at a density of  $5 \times 10^6$  cells per well in 6-well plates (SPL Life Science, Korea), and  $5 \times 10^5$  SCs grown in media containing an anticancer drug (DOX; dose, 0, 0.005, 0.05, and 0.5 µg/mL) were seeded onto 0.4-µm pore-sized Transwell inserts (SPL Life Science) for 48 h.

### Cell cycle analysis

TCs were washed with PBS and fixed with 70% ethanol at 4°C. The cells were then incubated with 500 µL of propidium iodide/RNase buffer (BD Biosciences, USA) for 30 min at room temperature. The samples were analyzed using flow cytometry (FACS Aria II, BD Biosciences).

**Table 1.** Sequences of PCR primers used in this study

Gene	Forward (5'-3')	Reverse (5'-3')	Reference
<i>cGAPDH</i>	TATGACGACATCAAGAAGGTAGTGA	GTAGCCAAATTCATTGTCATACCAG	[41]
<i>P-gp (ABCB1)</i>	CTATGCCAAAGCCAAAGTATC	GAGGGCTGTAGCTGTCAATC	[42]
<i>MRP1 (ABCC1)</i>	CGTGACCGTCGACAAGAACA	CACGATGCTGATGACCA	[42]
<i>BCRP (ABCG2)</i>	GGTATCCATAGCAACTCTCCTCA	GCAAAGCCGCATAACCAT	[42]
<i>HIF-1α</i>	ATGATGGTGACATGATTTACATTTCT	GTATTCTGCTCTTTACCCTTTTTTAC	[41]
<i>bFGF</i>	ACTGGCTTCTAAATGTGTTACTGAC	TAGCAGACATTGGAAGAAAAGTAT	[41]
<i>VEGF</i>	GAATGCAGACCAAAGAAAGATAGAG	GATCTTGACAAACAAATGCTTTCTC	[41]
<i>HGF</i>	AAATAAACATATCTGTGGAGGATCA	CAAGCTTCATAATCTTTCAAGTCTC	[41]

PCR, polymerase chain reaction; *cGAPDH*, cytosolic glyceraldehyde-3-phosphate dehydrogenase; *P-gp*, P-glycoprotein; *MRP1*, multi-drug resistance-related protein; *BCRP*, breast cancer resistance protein; *HIF-1α*, hypoxia-inducible factor 1; *bFGF*, basic fibroblast growth factor; *VEGF*, vascular endothelial growth factor; *HGF*, hepatocyte growth factor.

### Western blot analysis

Proteins were extracted from TCs using the pro-prep protein extraction solution (iNtRON Biotechnology). The protein concentrations were determined using the DC protein assay kit (Bio-Rad, USA). Approximately, 10  $\mu$ L of each protein was separated by sodium dodecyl sulfate-polyacrylamide gel electrophoresis. After electrophoresis, the proteins were transferred to a polyvinylidene difluoride membrane (Millipore, USA). The membranes were blocked with a blocking buffer containing 5% skim milk in Tris-buffered saline. Cell cycle arrest was detected using anti-procaspase-3 (dilution, 1:1,000; Santa Cruz Biotechnology) and anti-cyclin D1 antibody (dilution, 1:1,500; Cell Signalling Technology, USA). An anti- $\beta$ -actin antibody (dilution, 1:1,000; Santa Cruz Biotechnology) was used as a loading control. Immunoreactive bands were detected by chemiluminescence (Advansta, USA).

### Statistical analysis

All experiments were performed in triplicate and repeated three times. GraphPad prism (version 6.01) software (GraphPad, Inc., USA) was used for statistical analysis. The differences between two groups were analyzed using Student's *t*-tests, and differences among more than two groups were analyzed using one-way analysis of variance (ANOVA) followed by Bonferroni multiple comparison test. The results were presented as the mean value  $\pm$  SD. Differences with a value of  $p < 0.05$  were considered as statistically significant.

## RESULTS

### Interaction between TCs and SCs in hybrid 3D models

Our preliminary experiments revealed that the 3D culture model produced on the ultra-low attachment plate had an increased expression of angiogenic factors (*FGF*, *VEGF* and *HIF-1 $\alpha$* ) and tumor resistance genes (*BCRP*, *MRP1* and *P-gp*). Treatment with the anticancer drug DOX at 0.05  $\mu$ g/mL for 24 h, did not produce a significant reduction in cell viability of the 3D culture (**Supplementary Fig. 1A-E**). SCs derived from canine LN were characterized using flow cytometry. These cells exhibited high expression of CD90, CD73, CD29, CD34, CD44, and low CD45 expression. It was also confirmed that SCs can differentiate into adipocytes, chondrocytes, and osteocytes. Furthermore, most of the SCs were composed of endothelial cells (**Supplementary Fig. 2A-D**). Coculture of TCs and SCs using a 2D culture system confirmed that SCs play a role in supporting TCs (**Supplementary Fig. 3A and B**).

SCs and TCs were mixed and cultured on ultra-low adhesion plates to generate spheroids after 24 h (**Fig. 1A**). To study the interactions of SCs and GL-1 cells, we grew spheroids using different TC:SC ratios and measured their overall morphology and size. As seen in **Fig. 1B**, it was confirmed that the degree of condensation varied depending on the TC:SC ratio. It was confirmed that the hybrid model containing a 1:1 TC:SC ratio exhibited the best condensation. To clearly confirm the structure, H&E staining was performed by sectioning the center and 1/4 of the spheroid. This revealed that SCs and TCs were entangled together to form a single tissue (**Fig. 1C**). In addition, through immunofluorescence staining for VE-cad, CD79a and CD31, the matrix form composed of SCs and the arrangement of tumors and SCs were visualized. The results confirmed that CD79a positive GL-1 cells exist within a matrix consisting of SCs (**Fig. 1D**).

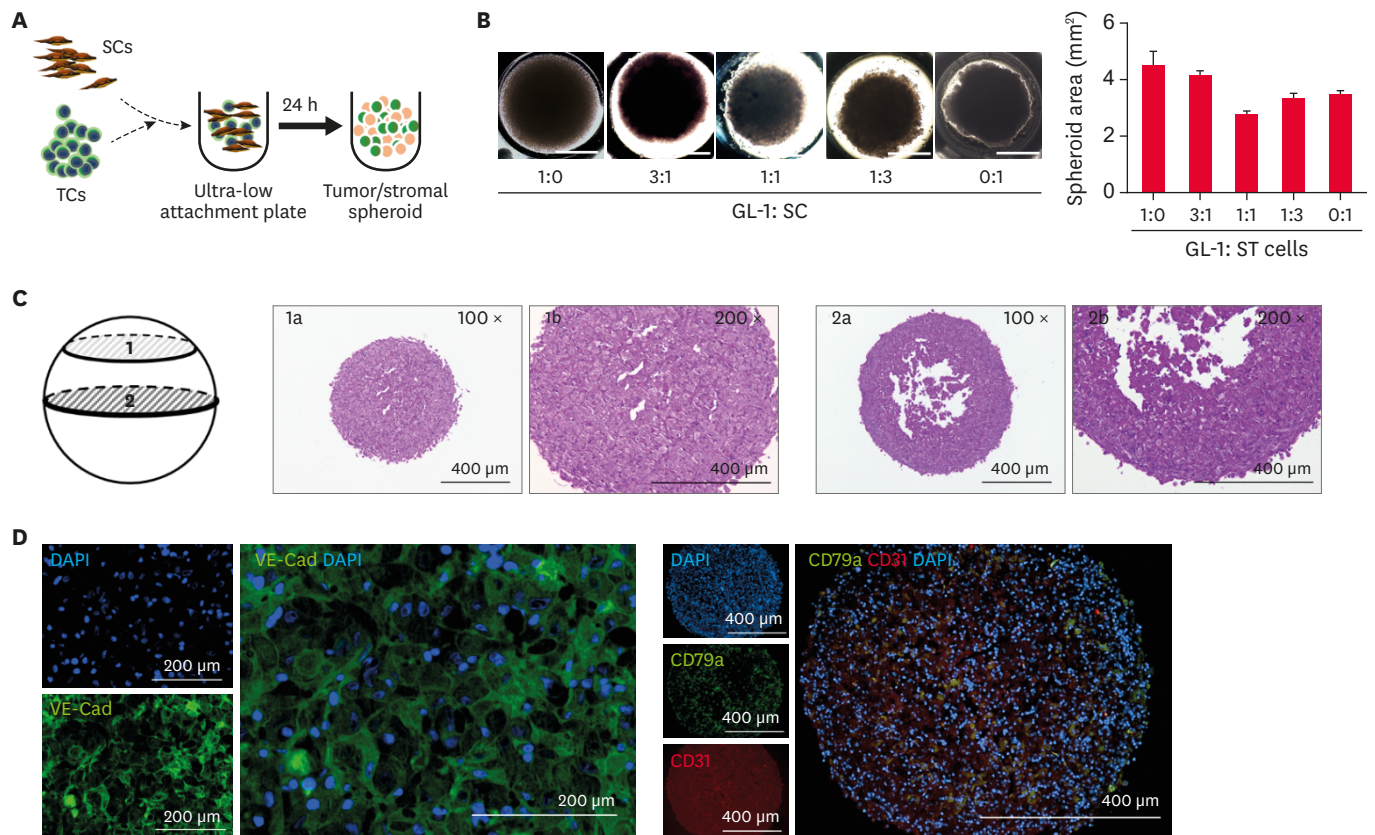


**Fig. 1.** Spheroid formation process and histological examination of TCs:SCs hybrid spheroid. (A) Illustration showing assembly of hybrid spheroid (B) Hybrid spheroid shape and size according to the ratio of TCs and SCs (white bar = 1 mm). (C) H&E staining in hybrid spheroid sections of TCs mixed with SCs at a 1:1 ratio. (D) Anti-VE-cadherin (green), anti-CD79a (green) and anti-CD31 (red) were used in the hybrid 3D culture model section to confirm cell-to-cell adhesion and TCs and SCs (blue = nuclei DAPI staining). The results are presented as the mean  $\pm$  SD of triplicate samples and are representative of 3 independent experiments. TC, tumor cell; SC, stromal cell; H&E, hematoxylin and eosin; 3D, 3-dimensional; DAPI, 4',6-diamidino-2-phenylindole.

### Hybrid 3D models treated with anticancer drugs

To show that spheroid sprouting depends on the anticancer drug concentration, spheroids (TC:SC of 1:1) were cultured in 96-well culture dishes under different concentrations of DOX for 5 days. The growth rate of spheroid was measured through Image J. Untreated spheroids were used as controls. As the concentration of the anticancer drugs increased, less cells were observed to sprout from the 3D model (Fig. 2).

### Cell viability of the tumor/stromal hybrid spheroid model under anti-cancer conditions

CCK analysis revealed that cell viability of cultures treated with DOX increased when cancer cells were cocultured with SCs (1:1 ratio of TC:SC) as opposed to when they were cultured alone in a 2D model. In addition, when SCs and TCs were cocultured directly, it was observed that the cell viability 3D cultures treated with anticancer drugs was higher than that of 2D cultures (Fig. 3).

### Growth factor expression by cross talk between TCs and SCs in coculture system

SCs, in addition to their role in maintaining tissue structure, also play an important role in maintaining the microenvironment for cancer growth, angiogenesis, and anticancer reactivity by interacting with TCs (Fig. 4A). Therefore, gene expression levels of growth and

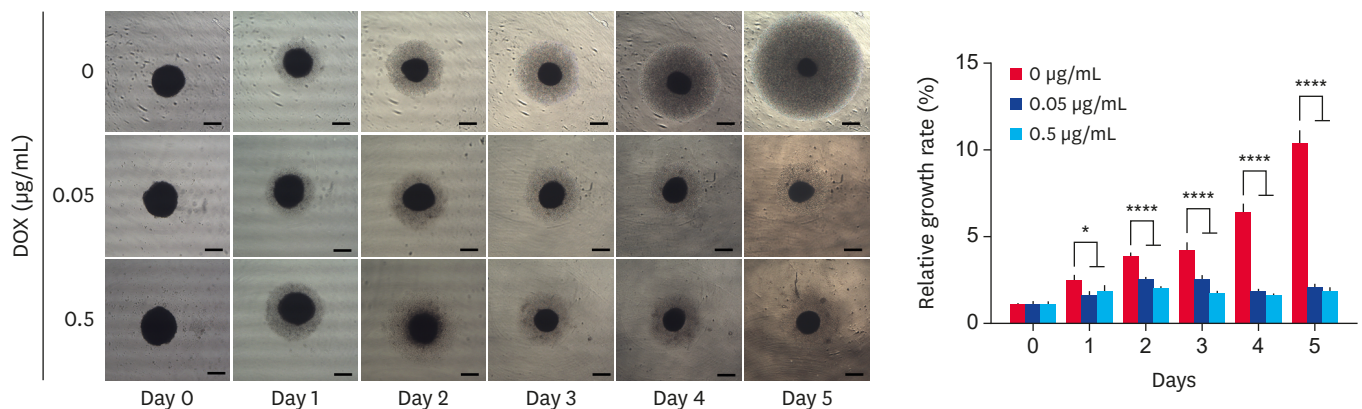


**Fig. 2.** Growth of tumor/stromal hybrid spheroid model under anti-cancer drug conditions (Dox; dose, 0, 0.05 and 0.5  $\mu\text{g/mL}$ ). The hybrid models formed at the ultra-low attachment were transferred to 96 well plate. Then, the models were cultured in different concentrations of anticancer agent, and morphology was observed ( $n=9$ , black bar = 1 mm). The results are presented as the mean  $\pm$  SD of triplicate samples of 3 independent experiments.

DOX, doxorubicin; ANOVA, analysis of variance.

\* $p < 0.05$ , \*\*\*\* $p < 0.0001$ , as determined by one-way ANOVA.

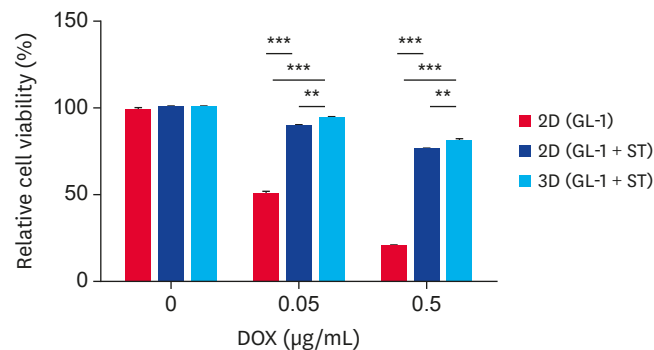


**Fig. 3.** Cell viability of tumor/stromal hybrid spheroid model under anti-cancer conditions (Dox; dose, 0, 0.05 and 0.5  $\mu\text{g/mL}$ ) compared to 2D culture cell model for 48 h. In co-cultured stromal cells and TCs, it was confirmed using CCK analysis that the cell survival rate of the 3D model was relatively higher than that of the 2D model under anticancer drug conditions. The results are presented as the mean  $\pm$  SD of triplicate samples of 3 independent experiments.

DOX, doxorubicin; TC, tumor cell; 2D, 2-dimensional; 3D, 3-dimensional; ANOVA, analysis of variance.

\* $p < 0.05$ , \*\* $p < 0.01$ , \*\*\* $p < 0.001$ , \*\*\*\* $p < 0.0001$ , as determined by one-way ANOVA.

angiogenesis factors such as *bFGF*, hepatocyte growth factor (*HGF*), *TGF- $\beta$* , and *VEGF* were analyzed in a coculture of TCs and SCs after 48 h in a transwell system. Coculture increased the expression of all factors except for *bFGF* in TCs (**Fig. 4B**). In the SCs, coculture with TCs caused similar gene expression changes (**Fig. 4C**). High expression of ABC-transporters, such as *P-gp* (*ABCB1*), *MRP1* (*ABCC1*), and *BCRP* (*ABCG2*) has been associated with both decreased sensitivity to cytotoxic agents, as well as a poor prognosis in several types of cancer in humans and dogs. TCs cocultured with SCs were found to have a significantly increased expression of multi drug resistance genes such as *P-gp*, *MRP1*, and *BCRP* as compared to monocultured TCs (**Fig. 4D**).

### Effect of LN SCs on the viability and cell cycle of TCs in coculture system

To identify tumor-stromal interactions that alter drug response, we initially used an *in vitro* coculture system that other groups had successfully used to evaluate tumor-stroma-drug interaction [22]. First, we investigated the effects of DOX on the viability of TCs (GL-1) and normal SCs. Treatment with a relatively low concentration (0.005  $\mu\text{g/mL}$ ) of DOX did not affect the viability of either cell type. However, incubation with 0.05  $\mu\text{g/mL}$  of DOX



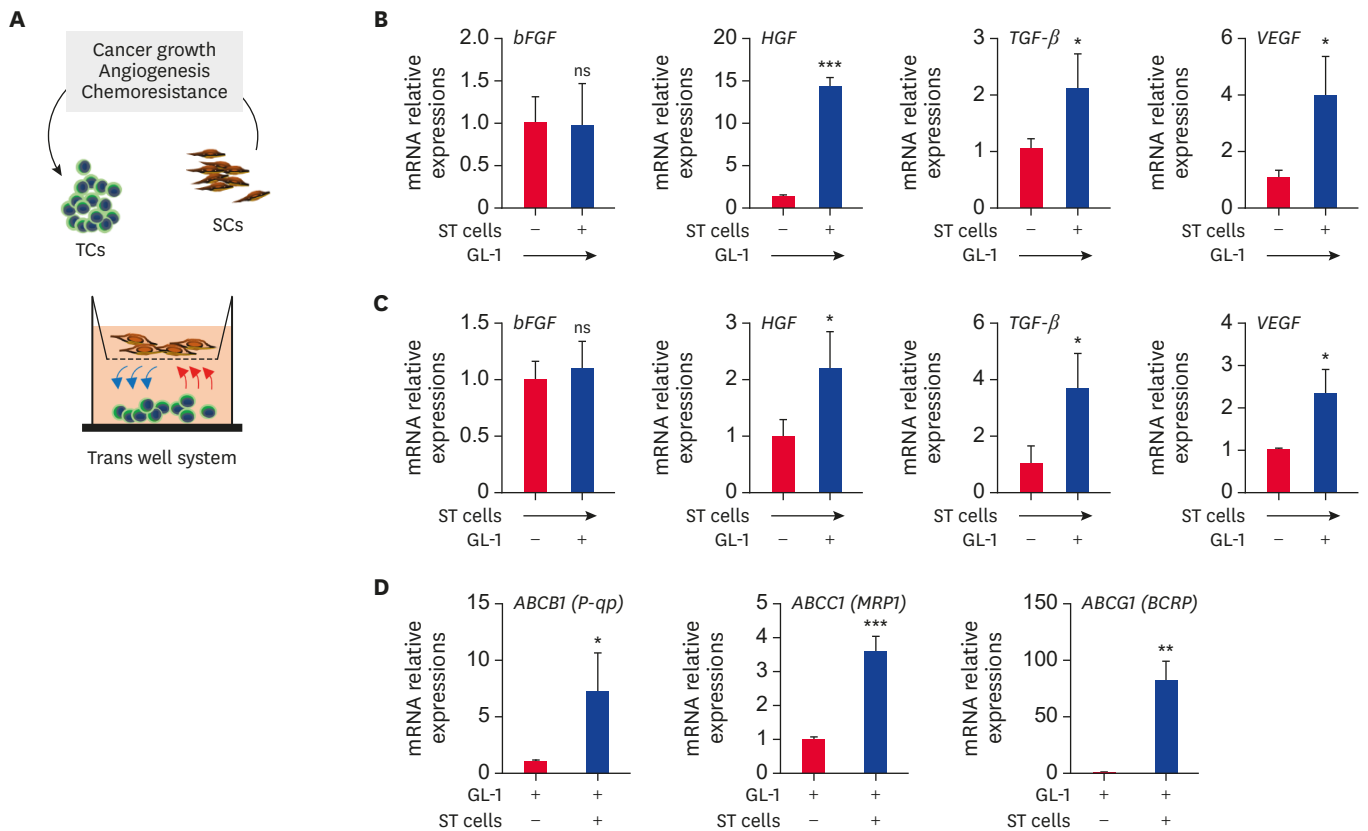


**Fig. 4.** Cross talk between TC and SC. (A) Schematic diagram depicting the cross talk between TCs (green) and 'normal' stroma cells (orange). (B) mRNA relative expression of Growth factors in TCs cocultured with or without SCs for 48 h. (C) mRNA relative expression of Growth factors in SCs cocultured with or without TCs for 48 h. (D) mRNA relative expression of multi-drug resistance gene (*MRP1*, *BCRP* and *P-gp*) in TCs cocultured with or without SCs for 48 h. The results are presented as the mean  $\pm$  SD of triplicate samples of three independent experiments. TC, tumor cell; SC, stromal cell; *MRP1*, multi-drug resistance-related protein; *BCRP*, breast cancer resistance protein; *P-gp*, P-glycoprotein; ANOVA, analysis of variance. \* $p < 0.05$ , \*\* $p < 0.01$ , \*\*\* $p < 0.001$ , \*\*\*\* $p < 0.0001$ , as determined by one-way ANOVA.

for 48 h decreased viability of GL-1 cells but did not affect SC viability (**Fig. 5A**). Therefore, when determining the effects of SCs on the activity of cancer cells, DOX concentrations non-cytotoxic to SCs (0–0.05  $\mu\text{g/mL}$ ) were used. To elucidate the underlying biochemical mechanisms involved in the regulation of apoptosis, the effect of SCs on caspase 3 protein levels and on annexin V staining was analyzed by western blotting and flow cytometry, respectively. As shown in **Fig. 5B**, procaspase-3 is upregulated in TCs cocultured with SCs, in the group treated with 0.05  $\mu\text{g/mL}$  DOX. In addition, cocultured TCs exhibited significantly less annexin V positive apoptotic cells as compared to monocultured controls, at treatments with 0.025 or 0.05  $\mu\text{g/mL}$  DOX (**Fig. 5C**). TCs were also harvested for cell cycle distribution analysis. The untreated TC population contained the highest portion of cells in the G0/G1 phase and the lowest in the G2/M phase. In comparison with the control, DOX treatment resulted in a significant accumulation of cells in the G2/M phase, which was accompanied by a decrease of cells in the G0/G1 phase. However, this was reduced significantly when cancer cells were cocultured with SCs (**Fig. 5D**).

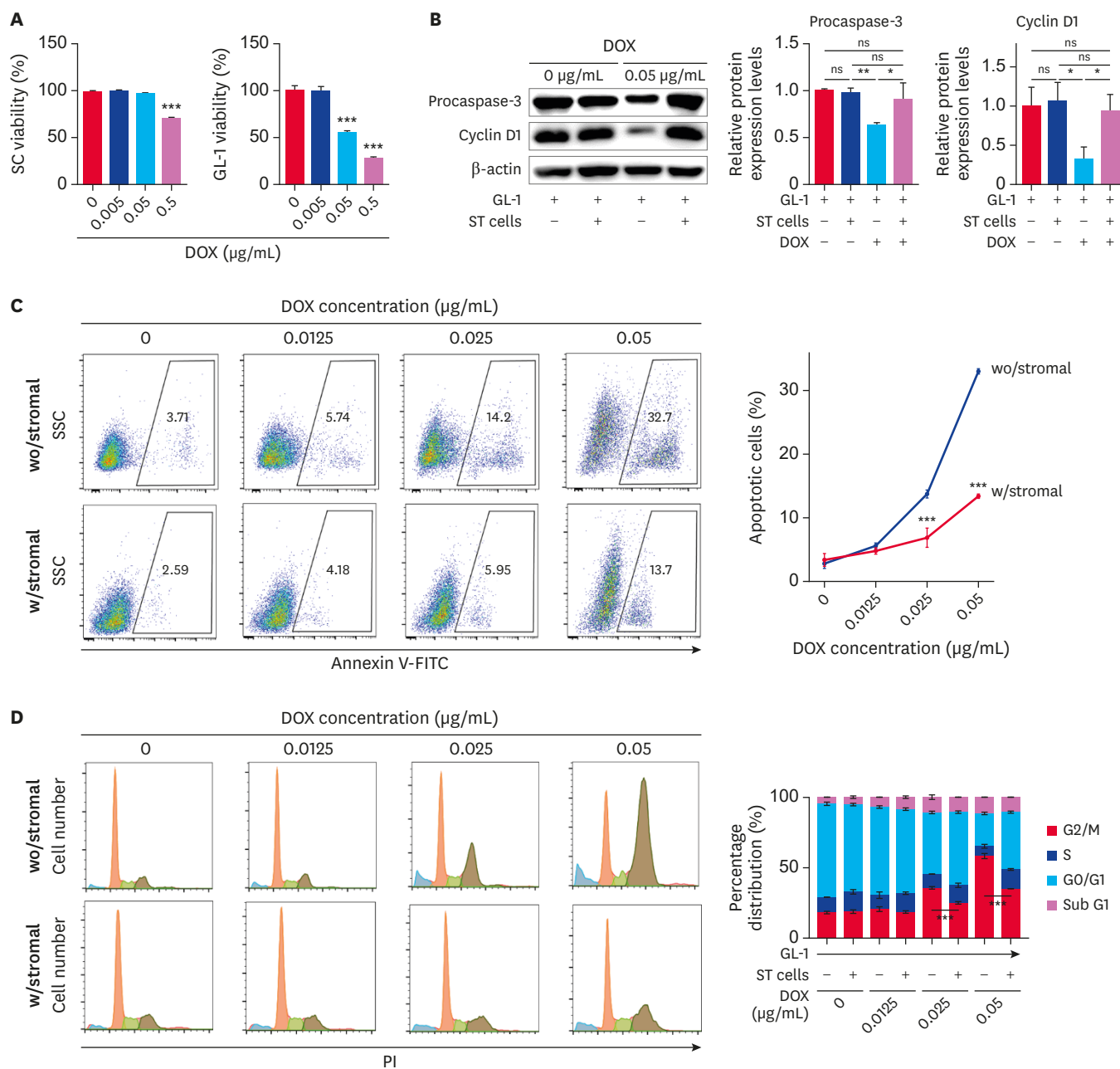


**Fig. 5.** Cross talk between TC and SC under anticancer drug. (A) Cell viability assay of GL-1 cultured with DOX (dose; 0, 0.005, 0.05, and 0.5 µg/mL) for 48 h. (B) Relative protein expression of procaspase-3 and cyclin D1 in TCs cocultured with or without stroma cells for 48 h. (C) Annexin V-FITC staining for TC apoptosis analysis (D) Cell cycle arrest assay using PI staining. The results are presented as the mean ± SD of triplicate samples of three independent experiments. TC, tumor cell; SC, stromal cell; DOX, doxorubicin; ANOVA, analysis of variance. \**p* < 0.05, \*\**p* < 0.01, \*\*\**p* < 0.001, \*\*\*\**p* < 0.0001, as determined by one-way ANOVA.

## DISCUSSION

In this study, LN-derived SCs were used to create a lymphocyte-SC hybrid 3D culture model, and these models showed reduced sensitivity to anticancer drugs compared with the 2D culture model.

It is now acknowledged that the tissue surrounding TCs has an important role in tumor progression and resistance [23]. As SCs play a crucial role in tumor resistance, different therapeutic approaches targeting tumor SCs have been investigated and are currently under evaluation, as reviewed in detail by several authors [24,25]. In particular, SCs in secondary lymphoid organs contribute to microenvironments by releasing chemokines and cytokines and by acting as a scaffold for cell trafficking. However, little is known about the role that LN SCs from canine LNs play in providing a supportive microenvironment to allow for lymphoid cell survival, activation, and stimulation [26].

First, we characterized plastic adherent cells derived from canine LNs as SCs based on their phenotype and their ability to differentiate into three mesodermal cell lineages. We distinguished endothelial cells from among the adherent cells based on CD31 and CD34 marker expression (**Supplementary Fig. 3**) [27]. CD31 is a single chain type-1 transmembrane protein that plays a role in adhesive interactions between adjacent endothelial cells as well as between leukocytes and endothelial cells [28]. CD34 is a single-chain transmembrane glycoprotein expressed on hematopoietic precursor cells and capillary endothelial cells. Moreover, these cells have the ability to regulate angiogenic factors such as *VEGF* [29].

In a previous study, tissue size and shape of the 3D culture model were controlled when using the ultra-low attachment plate [12]. However, we observed that the 3D culture of GL-1 exhibited weak aggregation. As lymphocytes are generally mobile, it is reasonable to predict that the SC substrate population will support their distribution and movement as a structural backbone within the LN.

Extracellular matrix containing SCs, which histologically often encapsulate TC clusters, can act as a barrier to protect tumor cells from therapeutic agents [30]. This causes a decrease in overall supply of oxygen, nutrients and metabolites [30]. Hypoxia and increased metabolic stress lead to suppression of apoptosis and activation of drug resistance pathways [31]. In the 3D hybrid spheroid model, the extracellular matrix composed of SCs was confirmed by VE cadherin staining [32]. In addition, CD79a-positive TCs were present in the ECM, which was composed of stromal cells.

As in humans, treatment of lymphoma in dogs consists of a multidrug chemotherapy protocol that includes, as a minimum, cyclophosphamide, DOX, vincristine, and prednisolone (of CHOP-protocol) [33]. Of these, DOX appears the most effective as a single agent [34]. Therefore, we explored the interaction between lymphoma cells and SCs to identify how this modulates the sensitivity to DOX, a commonly used chemotherapeutic.

In this study, sprouting of TCs from an ECM composed of SCs was decreased when treated with anticancer drugs. This demonstrates a major characteristic of the SC representing the protective properties against antitumor drugs in the body [35]. In addition, when using coculture of TCs with SCs in 2D culture, viability was increased when treated with anti-cancer drugs, and it was further increased in 3D culture. These results demonstrate that TC monocultures cannot recapitulate the *in vivo* tumor environment. Furthermore, 3D culture models supplemented with the SCs are even more representative of the *in vivo* tumor environment. However, the role of SCs in lymphoma has not been investigated in veterinary medicine.

Using transwell co-culturing system, we confirmed that the SCs interacted with TCs, increased the gene expression of growth factors, and altered multidrug resistance genes of GL-1 cells.

Furthermore, it was confirmed that SCs upregulated the expression of procaspase-3 in TCs treated with DOX. This means that SCs influence apoptosis in TCs. We also analyzed apoptosis in TCs via Annexin-V staining. Our data revealed that SCs reduced apoptosis of TCs by downregulating the expression of apoptosis-related genes in TCs treated with anticancer agents.

One limitation of our study is that 3D culture systems have not been used in studies to confirm the interaction of TCs and SCs. However, using the transwell coculture system, we confirmed that TCs and SCs influenced the sensitivity of tumors to anticancer drugs through the regulation of growth factor and drug resistance gene expression. The results of this study will be an important basis for creating a hybrid 3D culture model using SCs.

Growth-promoting signals in the microenvironment play a critical role in both normal and pathological tissues [36]. Previous studies have revealed that tumor SCs provide cancer cells with growth-promoting signals, involving growth factors, cytokines, and chemokines [37]. Growth factors, secreted by SCs into the microenvironment, promote tumor progression via stimulation of cellular growth, proliferation, and differentiation. In fact, various studies have shown that *FGF*, *HGF*, *TGF- $\beta$* , and *VEGF* are involved in cell cycle progression, angiogenesis, and proliferation of TCs in tumors [38]. It has also been found that various growth factors secreted by TCs also affect the growth of SCs around the tumor.

Although this study did not determine which factor acts as a key factor, in veterinary medicine, studies on the stimulation of growth factors between SCs and TCs are scarce. This study is significant because it is the first study that demonstrates that growth factor expression is affected in a coculture of TCs and SCs.

In addition, recent publications provide strong evidence that increased expression of growth factors in the tumor microenvironment contributes to chemoresistance. Li et al. [15] demonstrated that VEGF enhanced the expression of MRP1 at both the mRNA and protein levels, which increased the MDR in cancer cells. Deying et al. [39] showed that HGF contributed to cell proliferation and drug resistance by activating c-Met/PI3K/Akt and GRP78 signaling in cancer cells. Katsuno et al. [40] demonstrated that long-term TGF- $\beta$  treatment also increased resistance to anticancer drugs.

The data generated in this study validate those obtained in previous studies. Our data indicate that coculture of TCs with SCs upregulated expression of *P-gp*, *MRP1*, and *BCRP*, known as multidrug resistance genes.

Detailed mechanisms underlying the functional role of SCs in 3D cultures are still unclear, but these reports suggest that hybrid 3D cultures might be an effective strategy for modeling lymphoma *in vitro* to facilitate cancer research and therapy [23]. Further studies should aim at gaining a comprehensive understanding of the mechanisms of interaction between SCs and cancer cells, particularly the mechanisms by which SCs alter the primed state of cancer cells.

Primary cancer cells partially reproduce the natural *in situ* microenvironment of the disease, maintaining the crosstalk between malignant and healthy components. Such features are known to be involved in the variation in responses to therapies and in all the stages of the natural progression of malignant tumors, i.e., cancerogenesis, migration, progression, and metastatic dissemination. Therefore, primary cancer cells are considered the best platform for *in vitro* assay purposes. However, cancer cell lines are relatively easy to culture (basic media

requirements and simple culture protocols) and have a virtually infinite lifespan. Thus, they have been recognized by a majority of scientists as helpful in evaluating anticancer agents and confirming their mechanisms. For this reason, stable cancer cell lines have been considered a valuable tool in studying cancer biology and have been used in preclinical drug testing for many years. However, it is more challenging to elucidate all the characteristics of a TC line as compared to primary oncogenic cell lines.

Our study indicates that SCs derived from LNs aid in recapitulating *in vivo* tumor microenvironment in 3D cell culture models. These findings will provide basic data for modeling similar *in vivo* conditions in future drug evaluations.

In summary, the primary cause of unresponsiveness of tumors to antineoplastic drugs is the overexpression of drug resistance and antiapoptotic proteins in TCs. In addition, 2D and 3D monoculture models do not fully recapitulate the *in vivo* environment. Therefore, the challenge for developing novel targeted therapies is the establishment of *in vitro* models that better reflect *in vivo* conditions. An *in vitro* canine lymphoma 3D culture system was developed in the present study using the GL-1 lymphoma cell line and LN SCs. Such a model can be used as a reliable prediction method to assay mechanisms of action and efficacy of therapeutic agents.

## SUPPLEMENTARY MATERIALS

### Supplementary Fig. 1

Spheroid made of GL-1 cell lines (A) Scheme of the 3D culture protocol (B) Typical images of spheroid made of GL-1. The spheroids were prepared using 3D culture dish with 25 well array. Cell viability of spheroid, using a live/dead staining with Acridine orange (AO) and Propidium iodide (PI). Viable cells appear as green, while nonviable cells appears as red. Data are representative of three independent experiments. Scale bar = 400  $\mu\text{m}$  (C) Different gene expression between 2D and 3D cultures. Expression of growth factors and hypoxia factor in 2D and 3D cell culture models (D) Expression of drug resistance gene in 2D and 3D culture models. (E) Sensitivity of anti-cancer drug response in 2D and 3D culture model. Cell viability assay of GL-1 cultured with Doxorubicin (Dox; dose 0.05  $\mu\text{g}/\text{mL}$ ) for 24 h using AO/PI staining. The results are presented as the mean  $\pm$  SD of triplicate samples of three independent experiments.

[Click here to view](#)

### Supplementary Fig. 2

Canine LN SC characterization. (A) Scheme of LN SC isolation methods. (B) SC differentiate into adipocyte, osteocytes, chondrocytes. Data are representative of three independent experiments. Scale bars = 200  $\mu\text{m}$ . (C) Immunophenotype analysis by flow cytometry of SC (n = 3) They expressed CD90, CD73, CD29 and CD44, and these cells had less expression of hematopoietic markers such as CD45 and expressed endothelial cell markers such as CD34. Data are representative of three independent experiments (D) Dot plots show the gating of BEC (CD31+Gp38+) and LEC (CD31+Gp38-) from LN SC. They were classified into blood endothelial cells (BEC) and lymphatic endothelial cells (LEC) subpopulation according to CD31/Gp38 expressions. The results are presented as the mean  $\pm$  SD of triplicate samples. Three repeated experiments were conducted.

[Click here to view](#)

### Supplementary Fig. 3

TCs were direct cocultured with LN SCs. (A) TC were direct cocultured with LN SC. Immunofluorescent staining of GL-1 cell line attached to SC. GL-1 was attached to the SC to form a cluster. Data are representative of three independent experiments. (B) Cell adhesion assay of TC. After SC were attached to the dish at different concentrations (3 groups;  $2 \times 10^4$ ,  $1 \times 10^5$  and  $5 \times 10^5$  cells/mL), GL-1 was cocultured for 12 h at the same concentration ( $1 \times 10^6$  cells/mL). After gently washing with DPBS, GL-1 was stained with immunofluorescent staining (CD79a-FITC). The number of attached GL-I cells was counted. The results are presented as the mean  $\pm$  SD of triplicate samples of three independent experiments. Scale bars = 200  $\mu$ m.

[Click here to view](#)

## REFERENCES

1. Teske E. Canine malignant lymphoma: a review and comparison with human non-Hodgkin's lymphoma. *Vet Q.* 1994;16(4):209-219.  
[PUBMED](#) | [CROSSREF](#)
2. Uozurmi K, Nakaichi M, Yamamoto Y, Une S, Taura Y. Development of multidrug resistance in a canine lymphoma cell line. *Res Vet Sci.* 2005;78(3):217-224.  
[PUBMED](#) | [CROSSREF](#)
3. Flory AB, Rassnick KM, Erb HN, Garrett LD, Northrup NC, Selting KA, et al. Evaluation of factors associated with second remission in dogs with lymphoma undergoing retreatment with a cyclophosphamide, doxorubicin, vincristine, and prednisone chemotherapy protocol: 95 cases (2000–2007). *J Am Vet Med Assoc.* 2011;238(4):501-506.  
[PUBMED](#) | [CROSSREF](#)
4. Gavazza A, Lubas G, Valori E, Gugliucci B. Retrospective survey of malignant lymphoma cases in the dog: clinical, therapeutical and prognostic features. *Vet Res Commun.* 2008;32 Suppl 1:S291-S293.  
[PUBMED](#) | [CROSSREF](#)
5. Niu B, Scott AD, Sengupta S, Bailey MH, Batra P, Ning J, et al. Protein-structure-guided discovery of functional mutations across 19 cancer types. *Nat Genet.* 2016;48(8):827-837.  
[PUBMED](#) | [CROSSREF](#)
6. Ahn DH, Ciombor KK, Mikhail S, Bekaii-Saab T. Genomic diversity of colorectal cancer: changing landscape and emerging targets. *World J Gastroenterol.* 2016;22(25):5668-5677.  
[PUBMED](#) | [CROSSREF](#)
7. Breslin S, O'Driscoll L. Three-dimensional cell culture: the missing link in drug discovery. *Drug Discov Today.* 2013;18(5-6):240-249.  
[PUBMED](#) | [CROSSREF](#)
8. Xu X, Farach-Carson MC, Jia X. Three-dimensional *in vitro* tumor models for cancer research and drug evaluation. *Biotechnol Adv.* 2014;32(7):1256-1268.  
[PUBMED](#) | [CROSSREF](#)
9. Menshykau D. Emerging technologies for prediction of drug candidate efficacy in the preclinical pipeline. *Drug Discov Today.* 2017;22(11):1598-1603.  
[PUBMED](#) | [CROSSREF](#)
10. Benien P, Swami A. 3D tumor models: history, advances and future perspectives. *Future Oncol.* 2014;10(7):1311-1327.  
[PUBMED](#) | [CROSSREF](#)
11. Nath S, Devi GR. Three-dimensional culture systems in cancer research: focus on tumor spheroid model. *Pharmacol Ther.* 2016;163:94-108.  
[PUBMED](#) | [CROSSREF](#)
12. Shoval H, Karsch-Bluman A, Brill-Karniely Y, Stern T, Zamir G, Hubert A, et al. Tumor cells and their crosstalk with endothelial cells in 3D spheroids. *Sci Rep.* 2017;7(1):10428.  
[PUBMED](#) | [CROSSREF](#)
13. Langhans SA. Three-dimensional *in vitro* cell culture models in drug discovery and drug repositioning. *Front Pharmacol.* 2018;9:6.  
[PUBMED](#) | [CROSSREF](#)

14. DelNero P, Lane M, Verbridge SS, Kwee B, Kermani P, Hempstead B, et al. 3D culture broadly regulates tumor cell hypoxia response and angiogenesis via pro-inflammatory pathways. *Biomaterials*. 2015;55:110-118.  
[PUBMED](#) | [CROSSREF](#)
15. Li J, Wu X, Gong J, Yang J, Leng J, Chen Q, et al. Vascular endothelial growth factor induces multidrug resistance-associated protein 1 overexpression through phosphatidylinositol-3-kinase/protein kinase B signaling pathway and transcription factor specificity protein 1 in BGC823 cell line. *Acta Biochim Biophys Sin (Shanghai)*. 2013;45(8):656-663.  
[PUBMED](#) | [CROSSREF](#)
16. Di C, Zhao Y. Multiple drug resistance due to resistance to stem cells and stem cell treatment progress in cancer (Review). *Exp Ther Med*. 2015;9(2):289-293.  
[PUBMED](#) | [CROSSREF](#)
17. Correia AL, Bissell MJ. The tumor microenvironment is a dominant force in multidrug resistance. *Drug Resist Updat*. 2012;15(1-2):39-49.  
[PUBMED](#) | [CROSSREF](#)
18. Hanahan D, Coussens LM. Accessories to the crime: functions of cells recruited to the tumor microenvironment. *Cancer Cell*. 2012;21(3):309-322.  
[PUBMED](#) | [CROSSREF](#)
19. Khodarev NN, Yu J, Labay E, Darga T, Brown CK, Mauceri HJ, et al. Tumour-endothelium interactions in co-culture: coordinated changes of gene expression profiles and phenotypic properties of endothelial cells. *J Cell Sci*. 2003;116(Pt 6):1013-1022.  
[PUBMED](#) | [CROSSREF](#)
20. von Andrian UH, Mempel TR. Homing and cellular traffic in lymph nodes. *Nat Rev Immunol*. 2003;3(11):867-878.  
[PUBMED](#) | [CROSSREF](#)
21. Nakaichi M, Taura Y, Kanki M, Mamba K, Momoi Y, Tsujimoto H, et al. Establishment and characterization of a new canine B-cell leukemia cell line. *J Vet Med Sci*. 1996;58(5):469-471.  
[PUBMED](#) | [CROSSREF](#)
22. Gambara G, Gaebler M, Keilholz U, Regenbrecht CR, Silvestri A. From chemotherapy to combined targeted therapeutics: *in vitro* and *in vivo* models to decipher intra-tumor heterogeneity. *Front Pharmacol*. 2018;9:77.  
[PUBMED](#) | [CROSSREF](#)
23. Fang X, Sittadjody S, Gyabaah K, Opara EC, Balaji KC. Novel 3D co-culture model for epithelial-stromal cells interaction in prostate cancer. *PLoS One*. 2013;8(9):e75187.  
[PUBMED](#) | [CROSSREF](#)
24. Bahrami A, Hassanian SM, Khazaei M, Hasanzadeh M, Shahidsales S, Maftouh M, et al. The therapeutic potential of targeting tumor microenvironment in breast cancer: rational strategies and recent progress. *J Cell Biochem*. 2018;119(1):111-122.  
[PUBMED](#) | [CROSSREF](#)
25. Nunes AS, Barros AS, Costa EC, Moreira AF, Correia JJ. 3D tumor spheroids as *in vitro* models to mimic *in vivo* human solid tumors resistance to therapeutic drugs. *Biotechnol Bioeng*. 2019;116(1):206-226.  
[PUBMED](#) | [CROSSREF](#)
26. Margolin DA, Silinsky J, Grimes C, Spencer N, Aycock M, Green H, et al. Lymph node stromal cells enhance drug-resistant colon cancer cell tumor formation through SDF-1 $\alpha$ /CXCR4 paracrine signaling. *Neoplasia*. 2011;13(9):874-886.  
[PUBMED](#) | [CROSSREF](#)
27. Severino P, Palomino DT, Alvarenga H, Almeida CB, Pasqualim DC, Cury A, et al. Human lymph node-derived fibroblastic and double-negative reticular cells alter their chemokines and cytokines expression profile following inflammatory stimuli. *Front Immunol*. 2017;8:141.  
[PUBMED](#) | [CROSSREF](#)
28. Parums DV, Cordell JL, Micklem K, Heryet AR, Gatter KC, Mason DY. JC70: a new monoclonal antibody that detects vascular endothelium associated antigen on routinely processed tissue sections. *J Clin Pathol*. 1990;43(9):752-757.  
[PUBMED](#) | [CROSSREF](#)
29. Fiedler U, Christian S, Koidl S, Kerjaschki D, Emmett MS, Bates DO, et al. The sialomucin CD34 is a marker of lymphatic endothelial cells in human tumors. *Am J Pathol*. 2006;168(3):1045-1053.  
[PUBMED](#) | [CROSSREF](#)
30. Henke E, Nandigama R, Ergün S. Extracellular matrix in the tumor microenvironment and its impact on cancer therapy. *Front Mol Biosci*. 2020;6:160.  
[PUBMED](#) | [CROSSREF](#)

31. Rohwer N, Cramer T. Hypoxia-mediated drug resistance: novel insights on the functional interaction of HIFs and cell death pathways. *Drug Resist Updat*. 2011;14(3):191-201.  
[PUBMED](#) | [CROSSREF](#)
32. Nelson CM, Chen CS. VE-cadherin simultaneously stimulates and inhibits cell proliferation by altering cytoskeletal structure and tension. *J Cell Sci*. 2003;116(Pt 17):3571-3581.  
[PUBMED](#) | [CROSSREF](#)
33. Zandvliet M, Teske E, Schrickx JA. Multi-drug resistance in a canine lymphoid cell line due to increased P-glycoprotein expression, a potential model for drug-resistant canine lymphoma. *Toxicol In Vitro*. 2014;28(8):1498-1506.  
[PUBMED](#) | [CROSSREF](#)
34. Simon D, Moreno SN, Hirschberger J, Moritz A, Kohn B, Neumann S, et al. Efficacy of a continuous, multiagent chemotherapeutic protocol versus a short-term single-agent protocol in dogs with lymphoma. *J Am Vet Med Assoc*. 2008;232(6):879-885.  
[PUBMED](#) | [CROSSREF](#)
35. Pedersen SF, Hoffmann EK, Novak I. Cell volume regulation in epithelial physiology and cancer. *Front Physiol*. 2013;4:233.  
[PUBMED](#) | [CROSSREF](#)
36. Quail DF, Joyce JA. Microenvironmental regulation of tumor progression and metastasis. *Nat Med*. 2013;19(11):1423-1437.  
[PUBMED](#) | [CROSSREF](#)
37. da Cunha BR, Domingos C, Stefanini AC, Henrique T, Polachini GM, Castelo-Branco P, et al. Cellular interactions in the tumor microenvironment: the role of secretome. *J Cancer*. 2019;10(19):4574-4587.  
[PUBMED](#) | [CROSSREF](#)
38. Yuan Y, Jiang YC, Sun CK, Chen QM. Role of the tumor microenvironment in tumor progression and the clinical applications (Review). *Oncol Rep*. 2016;35(5):2499-2515.  
[PUBMED](#) | [CROSSREF](#)
39. Deying W, Feng G, Shumei L, Hui Z, Ming L, Hongqing W. CAF-derived HGF promotes cell proliferation and drug resistance by up-regulating the c-Met/PI3K/Akt and GRP78 signalling in ovarian cancer cells. *Biosci Rep*. 2017;37(2):37.  
[PUBMED](#) | [CROSSREF](#)
40. Katsuno Y, Meyer DS, Zhang Z, Shokat KM, Akhurst RJ, Miyazono K, et al. Chronic TGF- $\beta$  exposure drives stabilized EMT, tumor stemness, and cancer drug resistance with vulnerability to bitopic mTOR inhibition. *Sci Signal*. 2019;12(570):eaau8544.  
[PUBMED](#) | [CROSSREF](#)
41. Kim SM, Li Q, An JH, Chae HK, Yang JI, Ryu MO, et al. Enhanced angiogenic activity of dimethylxalylglycine-treated canine adipose tissue-derived mesenchymal stem cells. *J Vet Med Sci*. 2019;81(11):1663-1670.  
[PUBMED](#) | [CROSSREF](#)
42. Zandvliet M, Teske E, Schrickx JA, Mol JA. A longitudinal study of ABC transporter expression in canine multicentric lymphoma. *Vet J*. 2015;205(2):263-271.  
[PUBMED](#) | [CROSSREF](#)